Electronic Supplementary Information

Polymorphism of Porphyrin 2D Assemblies at the Liquid–Graphite Interface: Effect of Polar Solvent Additive and Flexible Spacer on the Face-On and Edge-On Type Molecular Arrangements

Kenya Adachi,[a] Takashi Hirose*[b] and Kenji Matsuda*[a]

[a]Department of Synthetic Chemistry and Biological Chemistry, Graduate School of Engineering, Kyoto University, Katsura, Nishikyo-ku, Kyoto 615-8510, Japan.

[b]Institute for Chemical Research, Kyoto University, Uji, Kyoto 611-0011, Japan.

E-mail: hirose@scl.kyoto-u.ac.jp (T.H.), kmatsuda@sbchem.kyoto-u.ac.jp (K.M.)

Contents:

1. Experimental Details

1.1 Materials and Synthesis

Unless specifically mentioned, reagents and solvents were obtained from commercial suppliers and used without further purification. All reactions were monitored by thin-layer chromatography carried out on 0.2 mm Merck silica gel plates (60F-254). Column chromatography was performed on silica gel (Nacalai Tesque, 70–230 mesh). ^{1}H and ^{13}C NMR spectra were recorded on a JEOL JNM-ECS400, JEOL JNM-Alpha500, or a JEOL JNM-ECA500 instrument. Proton chemical shifts are reported in ppm downfield from tetramethylsilane (TMS). Mass spectra were obtained by a JEOL JMS-MS700, JEOL JMS-HX110A, or a Thermo Fisher Scientific EXACTIVE mass spectrometer. Synthesis and characterization of compound **1-Fb** has been reported in literatures.[S1] Azeotropic mixture of formic acid/triethylamine (5/2) (triethylammonium formate, TEAF) was prepared as follows: triethylamine (22.4 mL, 16.3 g, 161 mmol) was slowly added to a stirred formic acid (15.1 mL, 18.4 g, 400 mmol) at 0 °C.[S2]

2-Fb with flexible ethylene spacer between amide group and the tetraphenylporphyrin (TPP) core was synthesized according the route shown in Scheme S1. 3-(4-formylphenyl)propanoic acid (**3**)[S3] was synthesized in 2 steps from 4-formylbenzonitrile by a Knoevenagel reaction with Meldrum's acid, followed by reduction of nitrile to aldehyde using Raney nickel. Acid-catalyzed condensation reaction of **3** with pyrrole in propionic acid afforded TPP-tetrapropionic acid **4** in 32% yield. 4-Fold amidation reaction of **4** with hexadecylamine successfully provided **2-Fb** in 27% yield.

Scheme S1. Synthesis of Compound 2-Fb

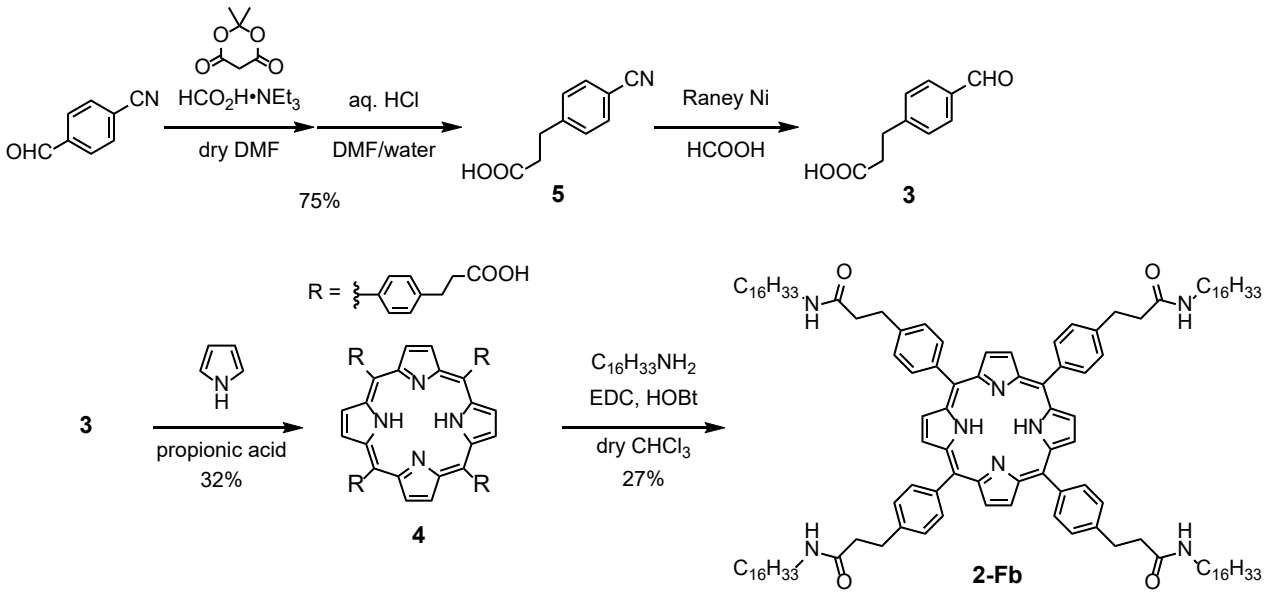

Synthesis of 3-(4-cyanophenyl)propanoic acid (**5**)

To a solution of **5** (780 mg, 5.95 mmol) in TEAF (30 mL) and DMF (30 mL) was added Meldrum's acid (884 mg, 5.85 mmol). The mixture was slowly heated to over 40 min and was stirred for 7h at the temperature. The resulting solution was then cooled to room temperature and the reaction was quenched by an addition of cooled water. The solution was acidified with concentrated aq. HCl until pH became 1. The reaction product was extracted with Et_2O. Combined organic layers were washed with water, dried over $MgSO_4$, filtered, and evaporated to give compound **5** (779 mg, 4.45 mmol, 75%) as a white solid.

^{1}H NMR (400 MHz, $CDCl_3$, δ): 2.73 (t, *J* = 7.6 Hz, 2H), 3.04 (t, *J* = 7.6 Hz, 2H), 7.34 (d, *J* = 8.4 Hz, 2H), 7.61 (d, *J* = 8.4 Hz, 2H).

Synthesis of 3-(4-formylphenyl)propanoic acid (**3**)

To a solution of **5** (1.00 g, 5.71 mmol) in 75% formic acid (15 mL) was added Raney Ni (999 mg). The stirred mixture was heated under reflux for 1.2 h. The mixture was filtered and washed with methanol and water. The filtrate was evaporated and then reprecipitated with water to give compound **3** (764 mg, 4.29 mmol, 75%) as a white solid.

^{1}H NMR (400 MHz, $CDCl_3$, δ): 2.74 (t, *J* = 7.6 Hz, 2H), 3.06 (t, *J* = 7.6 Hz, 2H), 7.40 (d, *J* = 8.0 Hz, 2H), 7.84 (d, *J* = 8.0 Hz, 2H), 9.99 (s, 1H); HRMS–ESI–orbitrap (*m*/*z*): $[M - H]^-$ calcd for $C_{10}H_9O_3^-$, 177.0557; found, 177.0552.

Synthesis of 5,10,15,20-tetrakis(4-(2-carboxyethyl)phenyl)porphyrin (**4**)

To refluxing propionic acid (20 mL) were added pyrrole (0.28 mL, 4.0 mmol) and **3** (712 mg, 4.00 mmol). After refluxing at 140 °C for 1 h, the reaction mixture was cooled to room temperature. After filtration the filter cake was washed with methanol and water to give compound **4** (298 mg, 32%) as a dark purple solid.

^{1}H NMR (400 MHz, DMSO, δ): −2.90 (brs, 2H), 2.84 (t, *J* = 7.6 Hz, 8H), 3.18 (t, *J* = 7.6 Hz, 8H), 7.67 (d, *J* = 7.6 Hz, 8H), 8.11 (d, *J* = 6.8 Hz, 8H). 8.80 (s, 8H); HRMS–ESI–orbitrap (*m*/*z*): $[M + H]^+$ calcd for $C_{56}H_{47}N_4O_8^+$, 903.3388; found, 903.3380.

Synthesis of 5,10,15,20-tetrakis(4-(N-hexadecylcarbamoylethyl)phenyl)porphyrin (**2-Fb**)

To a solution of compound **4** (110mg, 12.2 μmol) and trimethylamine (0.5 mL) in chloroform (30 mL) was added 1-hexadecylamine (290 mg, 1.20 mmol) and Water soluble carbodiimide (EDC) (186 mg, 0.97 mmol), 1,2,3,-benzotriazole-1-ol (HOBt) (129 mg, 0.95 mmol). The mixture was stirred for 54 hour at room temperature. The organic layer were extracted with aq. $NaHCO_3$ and washed with water. The organic layer was dried over $MgSO_4$ and evaporated to give a violet solid. The residue was purified by alumina column chromatography (DCM/MeOH = 99/1) to give compound **2-Fb** (60 mg, 3.3 μmol, 27%) as a violet solid.

^{1}H NMR ($CDCl_3$, 400 MHz, δ): 8.82 (s, 8H), 8.13 (d, *J* = 8.0 Hz, 8H), 7.59 (d, *J* = 7.6 Hz, 8H), 5.54 (t, *J* = 5.8 Hz, 4H), 3.36 (q., *J* = 7.6 Hz, 8H), 3.34 (q, *J* = 6.8 Hz, 8H), 2.78 (t, *J* = 7.8 Hz, 8H), 1.46–1.34 (m, 126H), 0.89–0.85 (m,12H), −2.78 (brs, 2H); ^{13}C NMR (101 MHz, $CDCl_3$, δ) 0.087, 14.21, 22.77, 27.08, 29.43, 29.71, 29.88, 31.79, 31.99, 38.70, 39.82, 120.01, 126.77, 134.86, 140.17, 140.52, 172.10; HRMS–MALDI–orbitrap (*m*/*z*): $[M + H]^+$ calcd for $C_{120}H_{179}N_8O_4^+$, 1796.4044; found, 1796.3977.

Synthesis of 5,10,15,20-tetrakis(4-(N-hexadecylcarbamoyl)phenyl)porphyrin (**1-Fb**)

To a solution of tetrakis(4-carboxyphenyl)porphyrin (100mg, 12.6 μmol) and trimethylamine (0.5 mL) in chloroform (30 mL) was added 1-hexadecylamine (243 mg, 1.01 mmol) and water soluble carbodiimide (EDC) (208 mg, 1.01 mmol), 1,2,3-benzotriazole-1-ol (HOBt) (137 mg, 1.01 mmol). The mixture was stirred for 19 hour at room temperature. The organic layer were extracted with aq. $NaHCO_3$ and washed with water. The organic layer was dried over $MgSO_4$ and evaporated to give a violet solid. The residue was purified by alumina column chromatography (DCM/MeOH = 99/1) to give compound **1-Fb** (64 mg, 3.8 μmol, 30%) as a violet solid.
^{1}H NMR ($CDCl_3$, 400 MHz, δ): 8.82 (s, 8H), 8.28 (d, *J* = 8.0 Hz, 8H), 8.16 (d, *J* = 8.4 Hz, 8H), 6.44 (t, *J* = 5.6 Hz, 4H), 3.65 (q., *J* = 6.8 Hz, 8H), 1.82–1.74 (m, 8H), 1.44–1.26 (m, 106H), 0.87 (t, *J* = 6.4 Hz,12H), −2.82 (brs, 2H); ^{13}C NMR (101 MHz, $CDCl_3$, δ): 0.078, 14.21, 22.77, 27.23, 29.44, 29.51, 29.80, 29.93, 32.00, 40.50, 119.44, 125.41, 134.54, 134.70, 145.13, 167.63.

1.2. STM Measurement

All STM experiments were performed at room temperature and ambient conditions. The STM images were acquired with an Agilent technologies 5500 scanning probe microscopes in the constant current mode. The STM tips used in this research were mechanically cut from a Pt/Ir wire (80/20, diameter 0.25 mm). Highly oriented pyrolytic graphite (HOPG) (ZYB grade, purchased from the ALLIANCE Biosystems Co.) was used as a substrate. To prepare a solution of **1-Fb** and **2-Fb** in octanoic acid and phenyloctane, **1-Fb** and **2-Fb** was dissolved in chloroform and then dispersed in each solution (chloroform/octanoic acid =1/19, chloroform/phenyloctane =1/19). A drop of the solution (10 μL) was deposited onto freshly cleaved HOPG using a micropipette, and the Pt/Ir tip was immersed into the solution and then the image was scanned. STM images were analyzed by using the graphite substrate as a calibration grid. The total STM scans were performed 2 times in order to determine an averaged surface coverage at a concentration of sample solution. The effect of thermal drift in STM measurements was corrected using two continuous STM images; one of the up- and down-scans of high-resolution STM images was stretched and the other was compressed along the vertical direction at the same scaling factor. Subsequently, the resulting set of images were sheared along the horizontal direction at the same shear angle with the opposite sign, so that the resulting unit cell parameters of the set of images are identical after the drift correction. The scaling factor and shear angle were estimated from the original unit cell parameters before the drift correction using the solver function in Microsoft Excel 2016. For an accurate analysis of lattice parameters (*a*, *b*, and α), evenly distributed grid lines were placed on a high resolution STM image so that all grid lines were consistent with the experimentally observed periodic pattern of molecular ordering. The length of the *a*- and *b*-axes, and the angle α were determined from the coordinates of intersection of the grid lines.

1.3. Molecular Modeling on Graphite Surface

The molecular ordering adsorbed on HOPG surface was modeled by a molecular mechanics/molecular dynamics (MM/MD) approach using BIOVIA Materials Studio 2018, Dassault Systems. The Dreiding force field implemented in the Forcite module was used for MM and MD calculations. The initial geometries were inspired from experimentally observed high resolution STM images for each ordering. For HOPG substrate, only one layer of graphene sheet (C–C bond length is 1.42 Å, flat geometry

having hexagonal symmetry, 150 × 150 superlattice of unit cell of graphene) was assumed using periodic boundary conditions (a = 36.9 nm, b = 36.9 nm, c = 5 nm (thickness of vacuum slab along the c-axis), $\alpha = \beta$ = 90°, γ = 120°). The Cartesian position of the graphene sheet was fixed during MM/MD calculation to suppress deformation/distortion of substrate. The face-on ordering consisting of 32 (8 × 4) molecules and the edge-on ordering of 48 (12 × 4) molecules on the graphene sheet were calculated to determine the unit cell parameters and adsorption energies.

2. Experimental Data

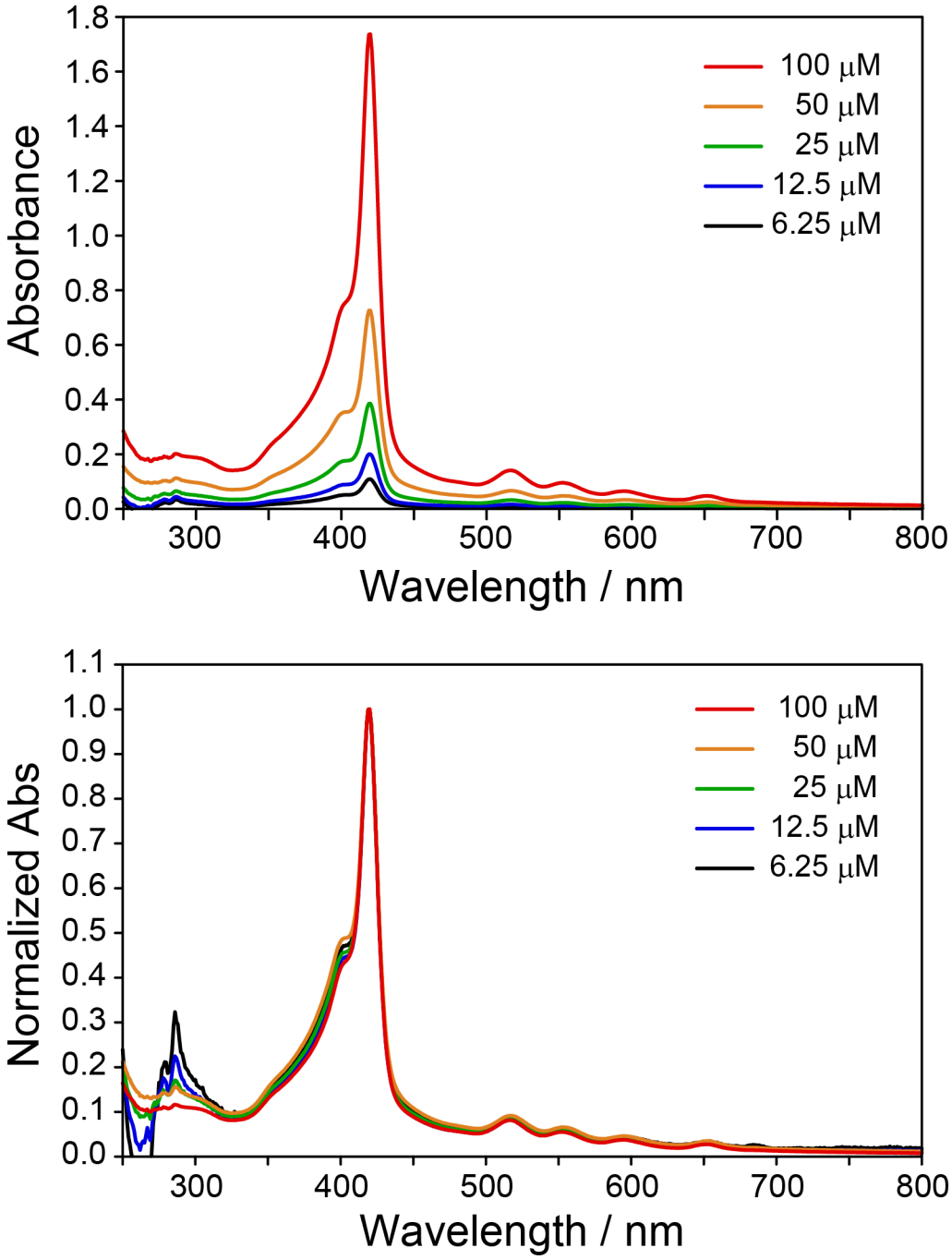

Figure S1. UV-vis absorption spectra of **1-Fb** in octanoic acid (optical path = 1 mm).

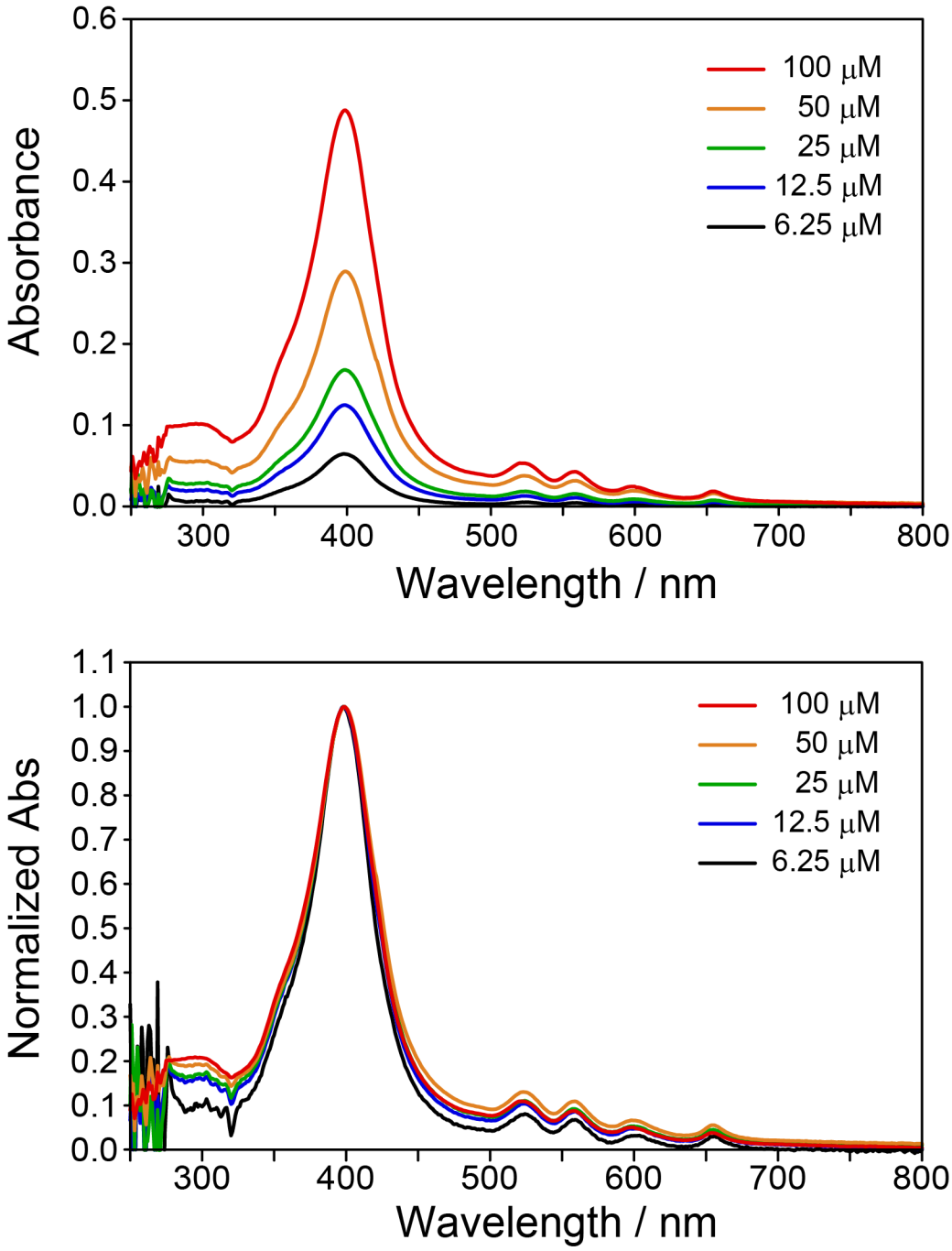

Figure S2. UV-vis absorption spectra of **1-Fb** in phenyl octane (optical path = 1 mm).

Table S1. Lattice parameters of the 2D orderings of **1-Fb** calculated by MM/MD model[a]

polymorph	unit cell parameters			
	a (nm)	*b* (nm)	*α* (°)	*S* (nm^2)[b]
face-on	3.86	1.86	75.1	6.94
edge-on	5.21	0.51	89.2	2.66

[a]Calculated using BIOVIA Materials Studio 2018, Dassault Systems. The Dreiding force field implemented in the Forcite module was used for MM/MD calculations. [b]The unit area occupied by one molecule of **1-Fb** on the surface.

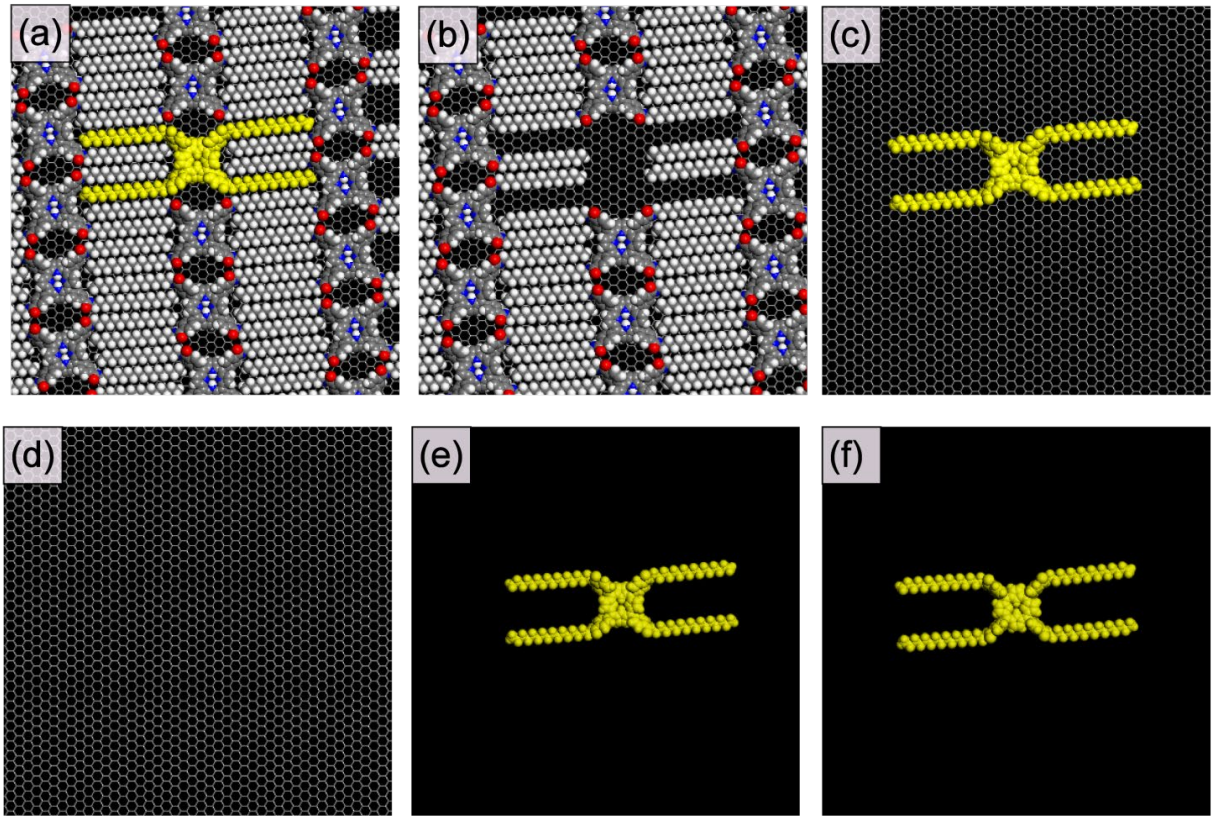

Figure S3. (a) Optimized molecular model of the 2-D ordering of face-on composed of 32 molecules of **1-Fb** on HOPG substrate using MM calculations (force field, Dreiding; quality, ultra-fine). The total energy of the structure was $E_{\text{ordering+HOPG}}$ = 2969.89 kcal·mol^{-1}. Molecular models for the single-point energy calculations: (b) one molecule of face-on ordering highlighted by yellow was removed from the 2-D ordering on HOPG (E_{defect}), (c) one molecule on HOPG ($E_{\text{monomer+HOPG}}$), (d) HOPG substrate only (E_{HOPG}), (e) one molecule without HOPG (E_{monomer}), and (f) one molecule optimized in gas phase without HOPG. For the calculation of edge-on, an optimized molecular model of the 2-D ordering composed of 48 molecules on HOPG substrate were used. The total energy of each structure and energy contributions are summarized in Tables S2 and S3. It is noted that the effect of entropy change and interaction with solvent molecules were not taken into account in the calculation.

Table S2. Total energy and each energy contribution of the face-on ordering of **1-Fb** on HOPG substrate.[a]

	$E_{\text{ordering+HOPG}}$[b] /kcal·mol^{-1}	E_{defect}[c] /kcal·mol^{-1}	$E_{\text{monomer+HOPG}}$[d] /kcal·mol^{-1}	E_{HOPG}[e] /kcal·mol^{-1}	E_{monomer}[f] /kcal·mol^{-1}
Total energy	2969.89	2936.04	131.17	0.00	337.32
Contributions to total energy					
Valence energy (diagonal terms)					
Bond	849.12	822.60	26.51	0.00	26.51
Angle	2815.13	2726.85	88.28	0.00	88.28
Torsion	1376.31	1333.82	42.49	0.00	42.49
Inversion	26.04	25.27	0.77	0.00	0.77
Non-bond energy					
Hydrogen bond	−14.96	−14.50	−0.47	0.00	−0.47
van der Waals	−2063.97	−1940.81	−25.89	0.00	179.73
Long range correction	−17.78	−17.19	−0.53	0.00	0.00

[a]Calculated with Forcite module implemented in Materials Studio 2018 in gas phase (force field, Dreiding; quality: ultra-fine) for 32 (8 × 4) molecules of **1-Fb** on one layer of graphene sheet in the gas phase. [b]Single-point energy of the molecular ordering with HOPG substrate. [c]Single-point energy of the molecular model in which one molecule was removed from the ordering on HOPG. [d]Single-point energy of one molecule on HOPG. [e]Single-point energy of HOPG substrate. [f]Single-point energy of one molecule without HOPG.

Table S3. Total energy and each energy contribution of the edge-on ordering of **1-Fb** on HOPG substrate.[a]

	$E_{\text{ordering+HOPG}}$[b] /kcal·mol^{-1}	E_{defect}[c] /kcal·mol^{-1}	$E_{\text{monomer+HOPG}}$[d] /kcal·mol^{-1}	E_{HOPG}[e] /kcal·mol^{-1}	E_{monomer}[f] /kcal·mol^{-1}
Total energy	8482.94	8407.70	262.71	0.00	358.17
Contributions to total energy					
Valence energy (diagonal terms)					
Bond	1213.91	1188.53	25.38	0.00	25.38
Angle	4265.81	4175.30	90.51	0.00	90.51
Torsion	3052.65	2984.72	67.94	0.00	67.94
Inversion	99.37	96.50	2.87	0.00	2.87
Non-bond energy					
Hydrogen bond	−242.40	−229.64	−0.79	0.00	−0.79
van der Waals	120.97	219.04	77.33	0.00	172.26
Long range correction	−27.37	−26.75	−0.53	0.00	0.00

[a]Calculated with Forcite module implemented in Materials Studio 2018 in gas phase (force field, Dreiding; quality: ultra-fine) for 48 (12 × 4) molecules of **1-Fb** on one layer of graphene sheet in the gas phase. [b]Single-point energy of the molecular ordering with HOPG substrate. [c]Single-point energy of the molecular model in which one molecule was removed from the ordering on HOPG. [d]Single-point energy of one molecule on HOPG. [e]Single-point energy of HOPG substrate. [f]Single-point energy of one molecule without HOPG.

Table S4. Adsorption energies for the face-on ordering of **1-Fb** on HOPG substrate[a]

	$E_{mol-sub}$[b] /kcal·mol^{-1}	$E_{mol-mol}$[c] /kcal·mol^{-1}	E_{ads}[d] /kcal·mol^{-1}	S[e] /nm^2	$E_{ads\_per\_area}$[f] /kcal·mol^{-1}·nm^{-2}
Total energy	−206.15	−48.66	−254.81	6.54	−38.95
Contributions to total energy					
Valence energy (diagonal terms)					
Bond	0.00	0.00	0.00	–	0.00
Angle	0.00	0.00	0.00	–	0.00
Torsion	0.00	0.00	0.00	–	0.00
Inversion	0.00	0.00	0.00	–	0.00
Non-bond energy					
Hydrogen bond	0.00	0.00	0.00	–	0.00
van der Waals	−205.62	−48.63	−254.25	–	−38.86
Long range correction	−0.53	−0.03	−0.56	–	−0.08

[a]Calculated from total energy and each energy contribution summarized in Table S2. [b]The molecule–substrate interaction energy calculated as follows, $E_{mol-sub} = E_{monomer+HOPG} - (E_{monomer} + E_{HOPG})$. [c]The molecule–molecule interaction energy calculated as follows, $E_{mol-mol} = \{E_{ordering+HOPG} - (E_{defect} + E_{monomer}) - E_{mol-sub}\}/2$. [d]The adsorption energy calculated as follows, $E_{ads} = E_{mol-sub} + E_{mol-mol}$. [e]The unit area occupied by one molecule of **1-Fb** on the surface determined by STM measurement at the PO/HOPG interface (a = 3.63 nm, b = 1.82 nm, α = 82°). [f]The adsorption energy per unit area calculated as follows, $E_{ads\_per\_area} = E_{ads}/S$. Other contributions such as (1) effects of entropy and (2) solvent interactions were not taken into account in this calculation.

Table S5. Adsorption energies for the edge-on ordering of **1-Fb** on HOPG substrate[a]

	$E_{mol-sub}$[b] /kcal·mol^{-1}	$E_{mol-mol}$[c] /kcal·mol^{-1}	E_{ads}[d] /kcal·mol^{-1}	S[e] /nm^2	$E_{ads\_per\_area}$[f] /kcal·mol^{-1}·nm^{-2}
Total energy	−95.46	−93.73	−189.19	2.30	−82.27
Contributions to total energy					
Valence energy (diagonal terms)					
Bond	0.00	0.00	0.00	–	0.00
Angle	0.00	0.00	0.00	–	0.00
Torsion	0.00	0.00	0.00	–	0.00
Inversion	0.00	0.00	0.00	–	0.00
Non-bond energy					
Hydrogen bond	0.00	−5.99	−5.99	–	−2.60
van der Waals	−94.94	−87.70	−182.63	–	−79.42
Long range correction	−0.53	−0.04	−0.57	–	−0.25

[a]Calculated from total energy and each energy contribution summarized in Table S3. [b]The molecule–substrate interaction energy calculated as follows, $E_{mol-sub} = E_{monomer+HOPG} - (E_{monomer} + E_{HOPG})$. [c]The molecule–molecule interaction energy calculated as follows, $E_{mol-mol} = \{E_{ordering+HOPG} - (E_{defect} + E_{monomer}) - E_{mol-sub}\}/2$. [d]The adsorption energy calculated as follows, $E_{ads} = E_{mol-sub} + E_{mol-mol}$. [e]The unit area occupied by one molecule of **1-Fb** on the surface determined by STM measurement at the PO/HOPG interface (a = 4.6 nm, b = 0.50 nm, α = 89°). [f]The adsorption energy per unit area calculated as follows, $E_{ads\_per\_area} = E_{ads}/S$. Other contributions such as (1) effects of entropy and (2) solvent interactions were not taken into account in this calculation.

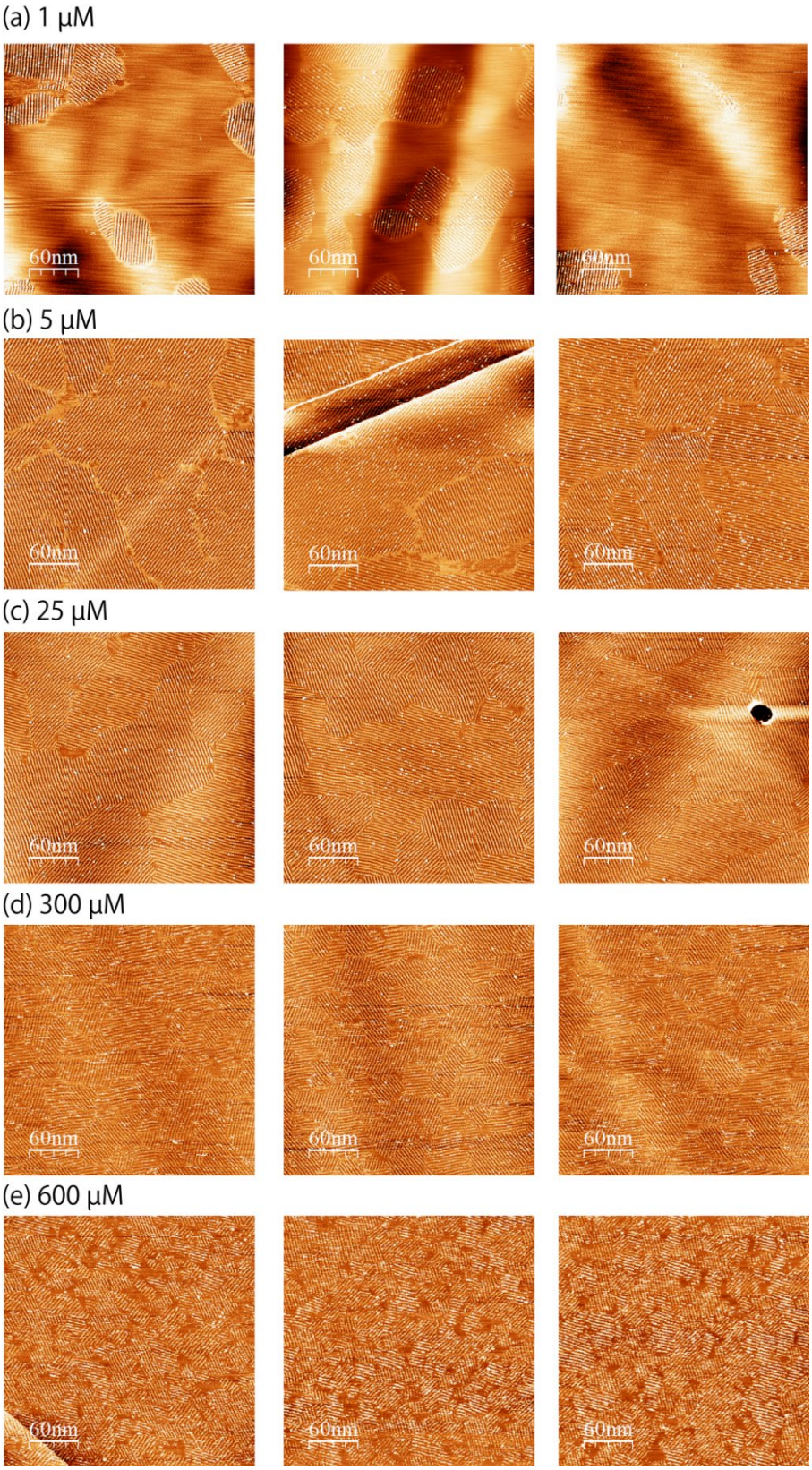

Figure S4. Representative STM images of **1-Fb** at different concentration at OA–HOPG interface (I_{set} = 20 pA, V_{bias} = −800 mV, 300 ×300 nm^2). The concentration of **1-Fb** was (a) 1 μM, (b) 5 μM, (c) 25 μM, (d) 300 μM, and (e) 600 μM respectively.

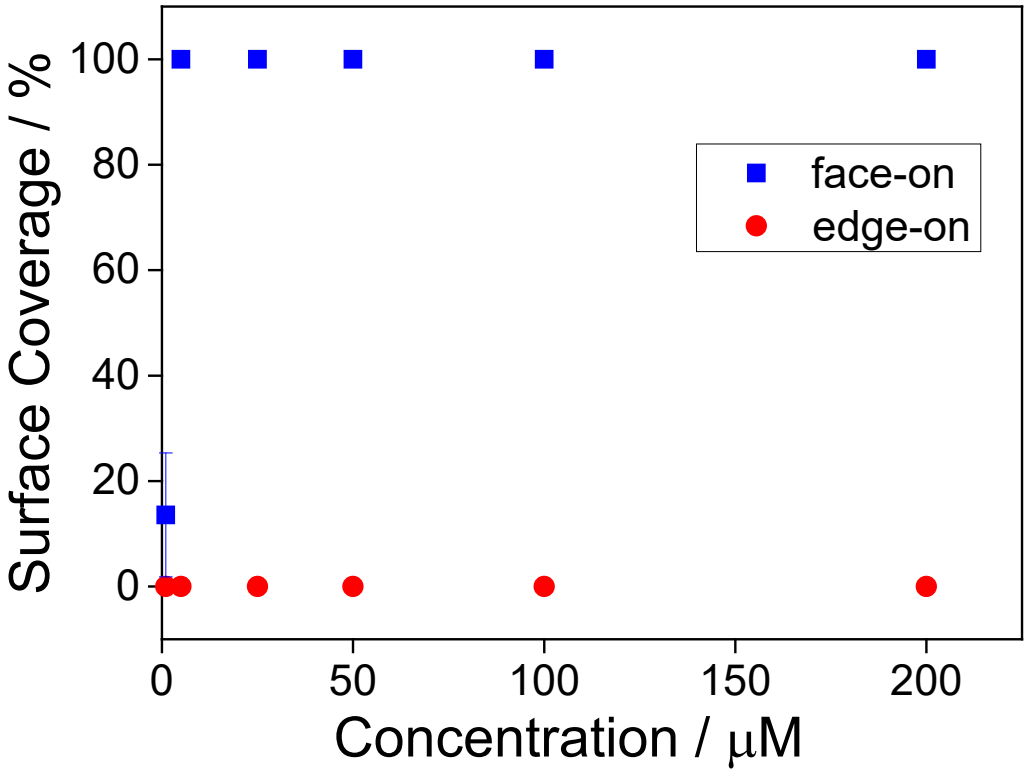

Figure S5. Surface coverage plot of **1-Fb** at the OA–HOPG interface depending on concentration. Blue square and red circle represent the face-on and edge-on orderings, respectively.

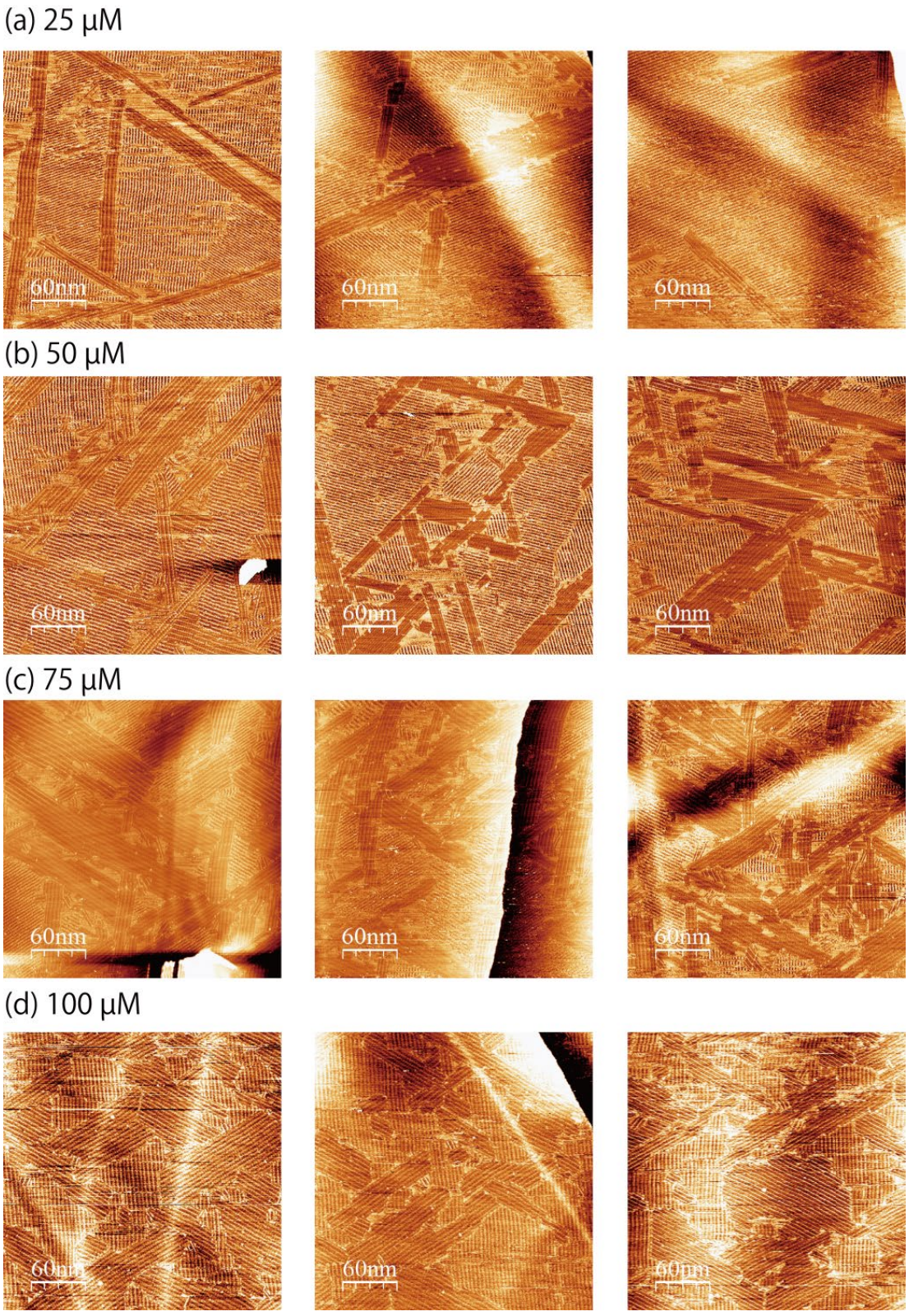

Figure S6. Representative STM images of **1-Fb** at different concentration at PO–HOPG interface (I_{set} = 20 pA, V_{bias} = −800 mV, 300 ×300 nm^2). The concentration of **1-Fb** was (a) 25 μM, (b) 50 μM, (c) 75 μM, and (d) 100 μM respectively. The statistical data to determine the averaged surface coverage of 2D ordering at a concentration was summarized in Table S6.

Table S6. Concentration dependence of surface coverage for the **1-Fb** using PO as a liquid phase[a]

entry	10 μM		25 μM		50 μM		75 μM		100 μM		150 μM	
	f [b]	e [c]	f [b]	e [c]	f [b]	e [c]	f [b]	e [c]	f [b]	e [c]	f [b]	e [c]
1	14.2	0.0	67.6	21.6	39.1	49.0	8.9	82.5	0	100	0	100
2	17.4	4.1	66.5	17.8	42.5	36.7	14.9	79.3	0	100	0	100
3	35.8	1.8	50.4	27.3	53.5	34.5	16.4	75.3	0	100	0	100
4	4.5	3.2	48.2	23.2	39.6	42.4	18.6	74.4	0	100	0	100
5	10.7	2.0	78.0	9.4	37.7	37.4	16.4	76.1	0	100	0	100
mean /%	16.5	2.2	58.2	22.5	42.5	40.0	15.0	77.5	0	100	0	100
SD[d] / %	11.8	1.6	10.3	3.9	6.4	5.8	3.7	3.3	0	0	0	0

[a]Obtained from STM measurements at the phenyloctane (PO)–HOPG interface. [b]Surface coverage of face-on type ordering. [c]Surface coverage of edge-on type ordering. [d]SD: Standard deviation.

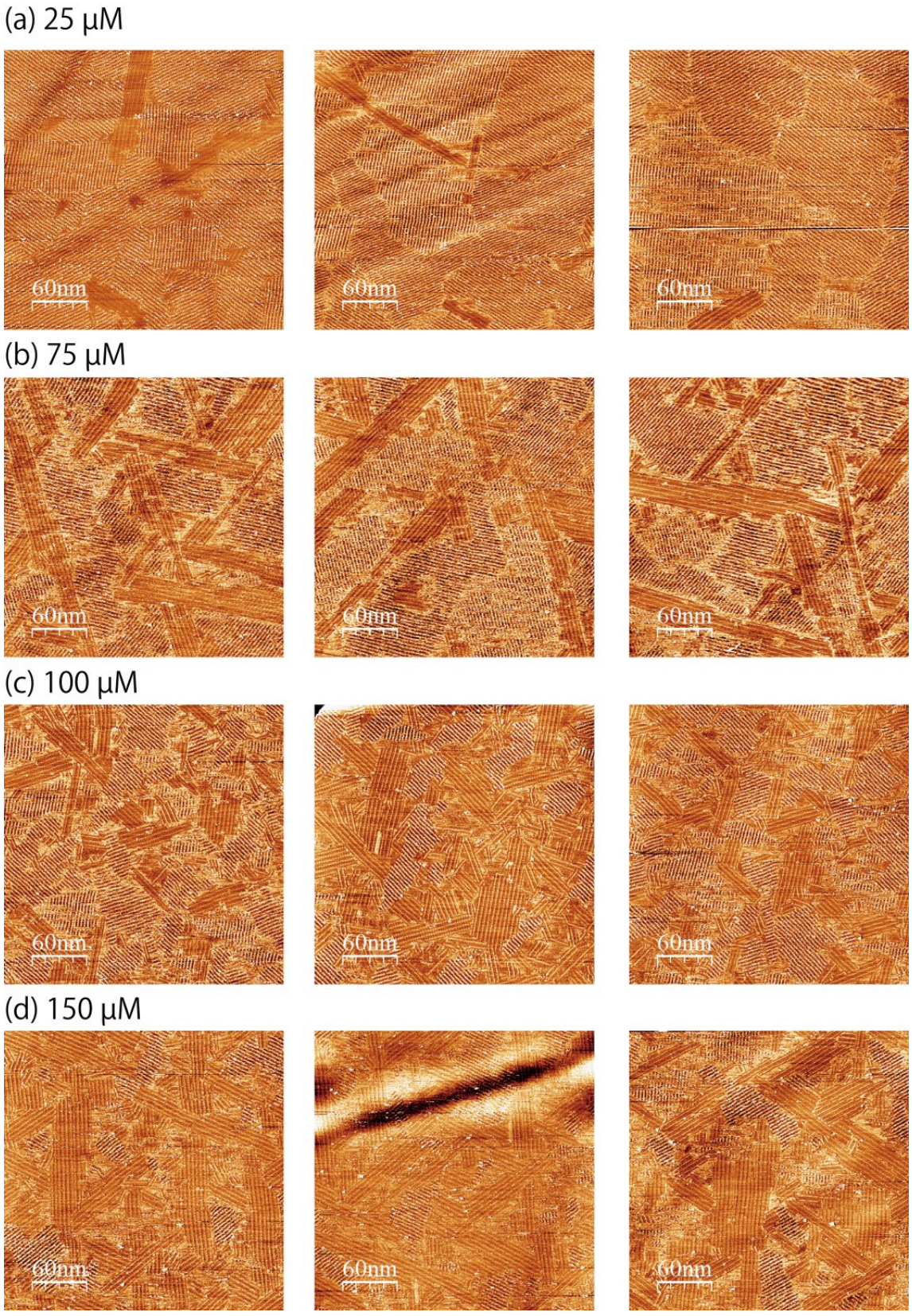

Figure S7. Representative STM images of **1-Fb** at different concentration at mixed solvent of OA/PO = 0.5/99.5 (v/v)–HOPG interface (I_{set} = 20 pA, V_{bias} = −800 mV, 300 ×300 nm^2). The concentration of **1-Fb** was (a) 25 μM, (b) 75 μM, (c) 100 μM, and (d) 150 μM respectively. The statistical data to determine the averaged surface coverage of 2D ordering at a concentration was summarized in Table S7.

Table S7. Concentration dependence of surface coverage for **1-Fb** using OA/PO (0.5/99.5 v/v) mixture[a]

entry	5 μM		15 μM		25 μM		50 μM		75 μM		100 μM		125 μM		150 μM	
	f [b]	e [c]	f [b]	e [c]	f [b]	e [c]	f [b]	e [c]	f [b]	e [c]	f [b]	e [c]	f [b]	e [c]	f [b]	e [c]
1	8.4	0.0	88.3	3.7	90.8	7.0	79.1	18.3	72.5	27.5	44.8	26.3	20.6	48.0	21.7	72.3
2	31.6	0.0	96.6	0.0	94.5	3.5	81.7	12.6	81.7	18.3	42.3	29.4	32.6	44.0	18.0	77.4
3	17.9	0.0	99.1	0.26	93.9	4.6	80.0	15.2	65.6	34.3	43.9	25.1	22.7	46.1	11.5	83.9
4	37.9	0.0	89.1	1.7	90.3	8.3	82.3	13.9	73.4	26.6	41.8	22.0	21.5	44.1	14.0	79.7
5	16.5	0.0	89.5	0.41	94.4	3.2	80.4	12.8	69.4	30.6	31.2	21.3	32.7	37.2	15.4	80.2
6	49.1	0.0	82.4	1.2	96.2	3.7	80.5	7.9	69.4	30.6	30.1	24.3	18.6	50.5	23.3	73.3
7	24.2	0.0	92.8	1.4	94.6	3.8			74.1	25.8	36.7	28.0	22.5	39.7	14.3	76.9
8	51.4	0.0	92.6	1.5	97.1	1.5			64.2	33.4					13.8	77.9
9	30.8	0.0			95.8	2.3										
10	48.4	0.0			97.4	0.9										
11					94.4	3.1										
Mean /%	31.6	0.0	91.3	1.3	94.5	3.8	80.7	13.4	71.3	28.4	38.8	25.2	24.5	44.2	16.5	77.7
SD / %	15	0.0	5.2	1.2	2.3	2.2	1.2	3.4	5.5	5.1	5.9	3.0	5.8	4.6	4.1	3.7

[a]Obtained from STM measurements at liquid–HOPGinterface where a mixed solvent of octanoic acid (OA)/phenyloctane (PO) = 0.5/99.5 (v/v) was used as a liquid phase. [b]Surface coverage of face-on type ordering. [c]Surface coverage of edge-on type ordering. [d]SD: Standard deviation.

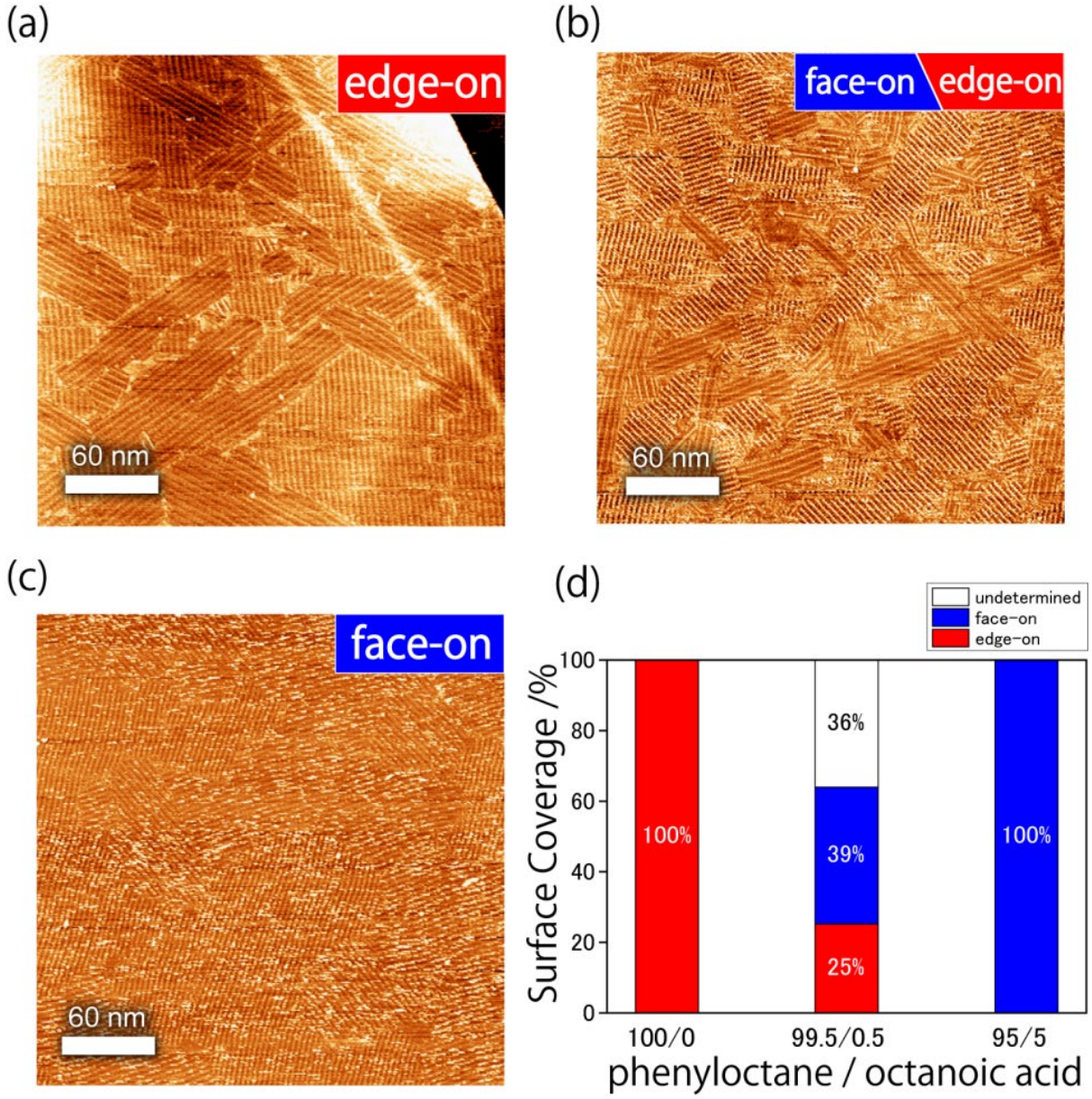

Figure S8. Representative STM images (I_{set} = 20 pA, V_{bias} = −800 mV, 300 ×300 nm^2) of **1-Fb** at mixed solvent of OA/PO (a) 0/100, (b) 0.5/99.5, and (c) 5/95 (v/v) respectively. The concentration of **1-Fb** was 100 μM. (d) Bar graph showing fractional surface coverage depending on the fraction of the two solvents.

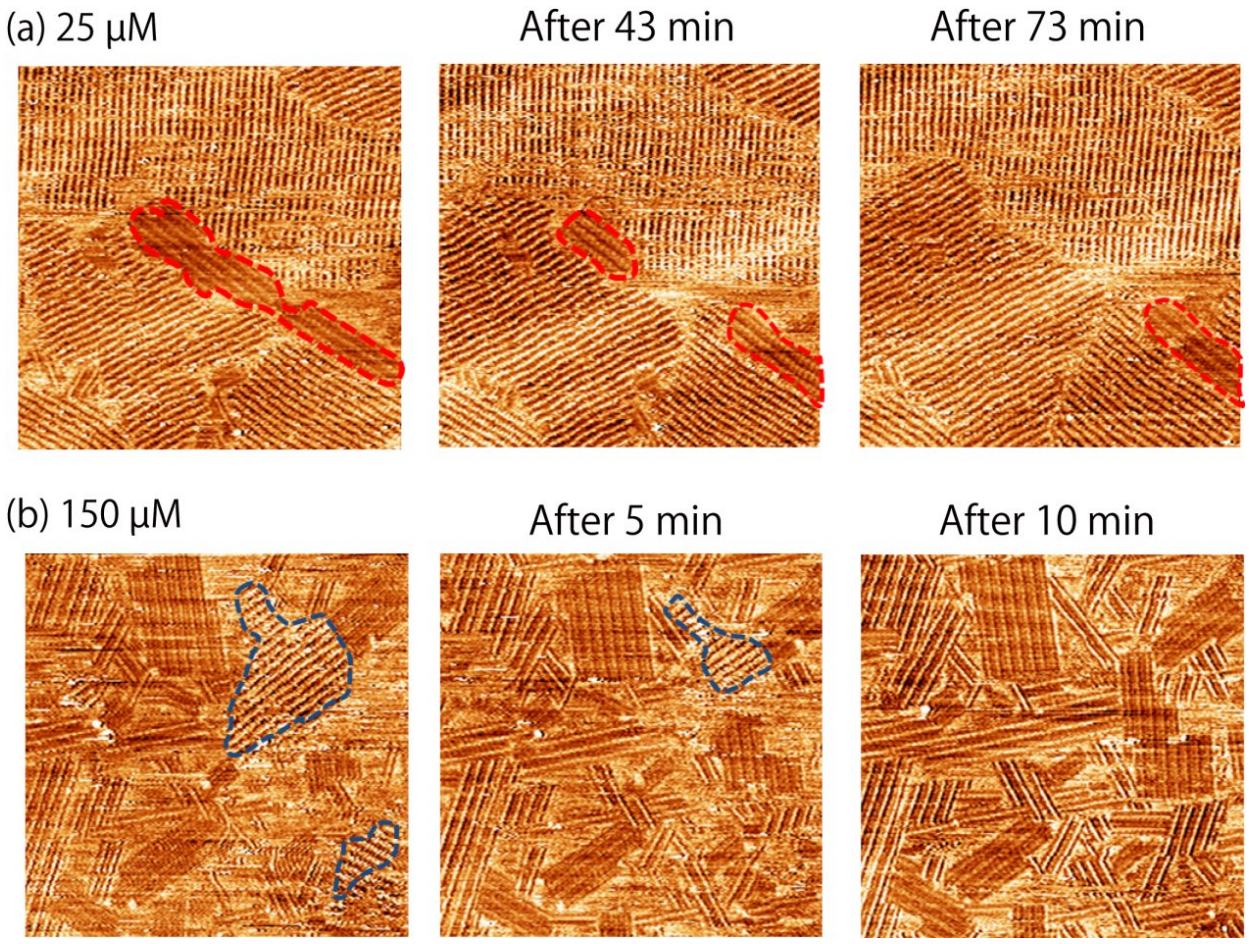

Figure S9. Real-time STM images (I_{set} = 20 pA, V_{bias} = −800 mV, 150 × 150 nm^2) of **1-Fb** at mixed solvent of OA/PO = 0.5/99.5. (a) Concentration of **1-Fb** was 25 μM. Red dashed line denotes the surface area in which the edge-on ordering was clearly observed. (b) Concentration of **1-Fb** was 150 μM. Blue dashed line denotes the surface area in which the face-on ordering was clearly observed. Interestingly, timescale of the disappearance of edge-on ordering domains (at 25 μm, more than 70 min) was much slower than that of the face-on ordering (at 150 μm, within 10 min). This is likely attributed to a strong molecule–molecule interactions in the edge-on arrangement with the π-π staking structure of porphyrin cores, which could slow down the rate of desorption at the boundary of ordered domains.

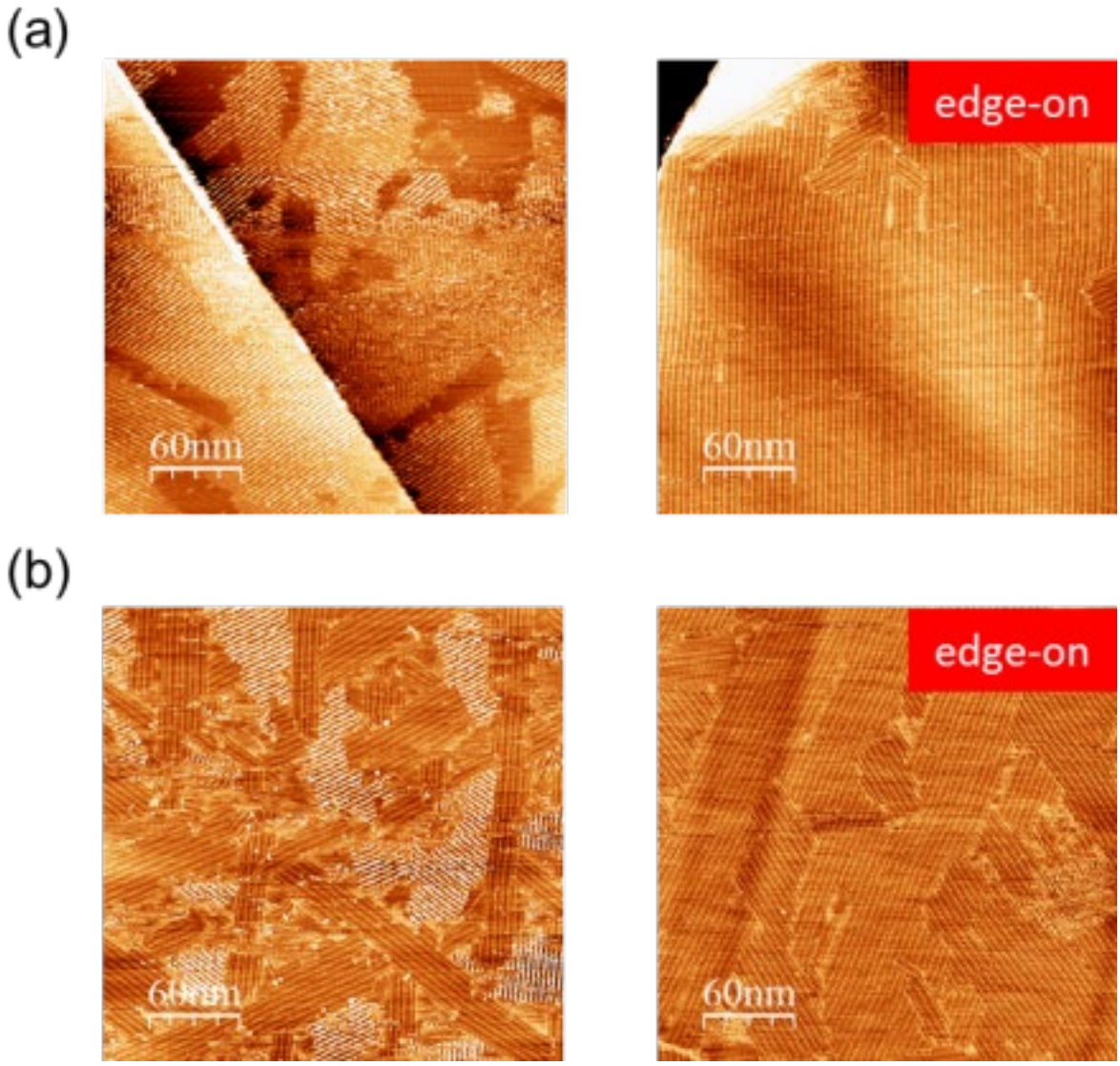

Figure S10. STM images (I_{set} = 20 pA, V_{bias} = −800 mV, 300 × 300 nm^2) of **1-Fb** at mixed solvent of OA /PO = 0.5/99.5. Concentration of **1-Fb** was (a) 50 μM and (b) 125 μM. Left images represent 2D ordering formed before annealing, i.e., STM images were recorded just after deposition of solution on HOPG substrate. Right images represent those after annealing at 60 °C for several minutes. All STM images were recorded at room temperature. It is noted that the size of 2D ordering domains significantly depended both on annealing treatment and concentration condition; (1) the domain size got clearly larger than STM scan size (> 300 × 300 nm^2) after annealing at 50 μM, and (2) the domain size tended to be small at high concentrations even after annealing at 60 °C.

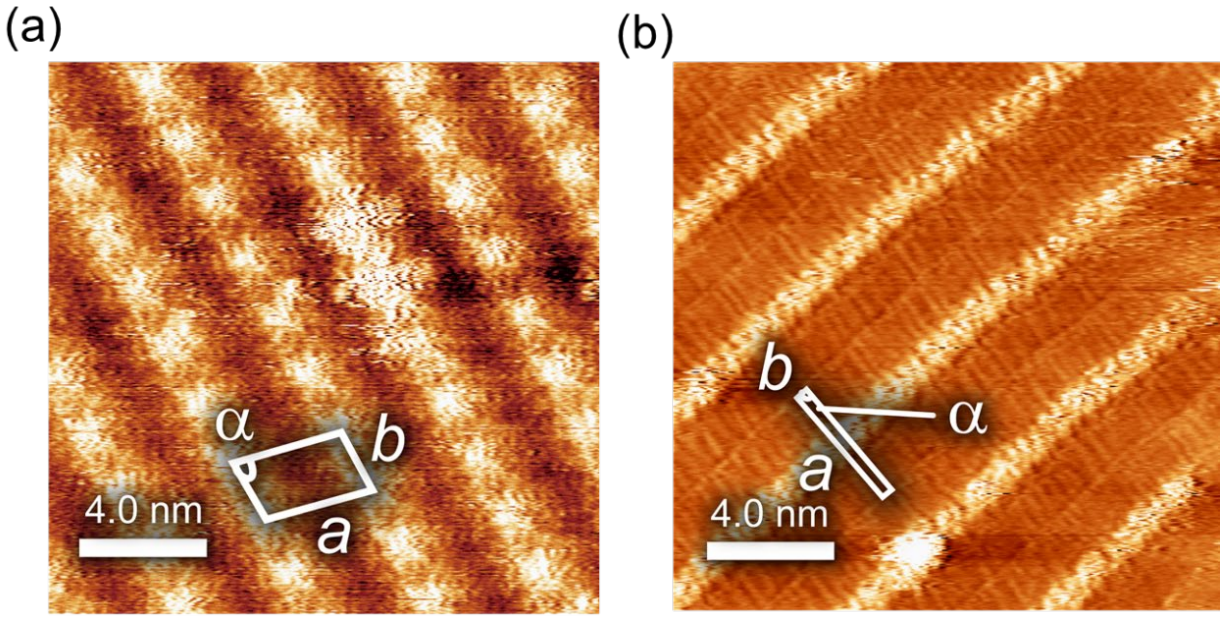

Figure S11. High-resolution STM images of **2-Fb** at the (a) octanoic acid– and (b) phenyloctane–graphite interface (c = 100 μM, I_{set} = 20 pA, V_{bias} = −0.80 V).

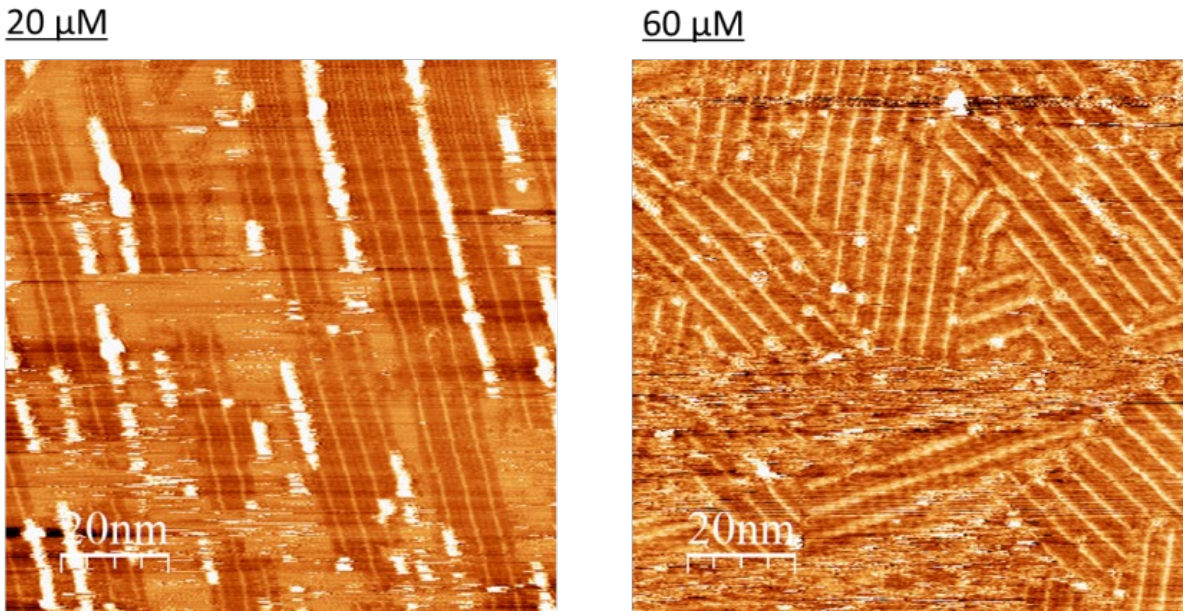

Figure S12. Representative STM images of **2-Fb** at the PO–HOPG interface at concentrations of 20 μM (left) and 60 μM (right) (I_{set} = 20 pA, V_{bias} = −800 mV, 100 × 100 nm^2). The edge-on ordering was exclusively observed for **2-Fb** even at low concentration, i.e., c = 20 μM, where surface coverage was not saturated.

3. NMR Data

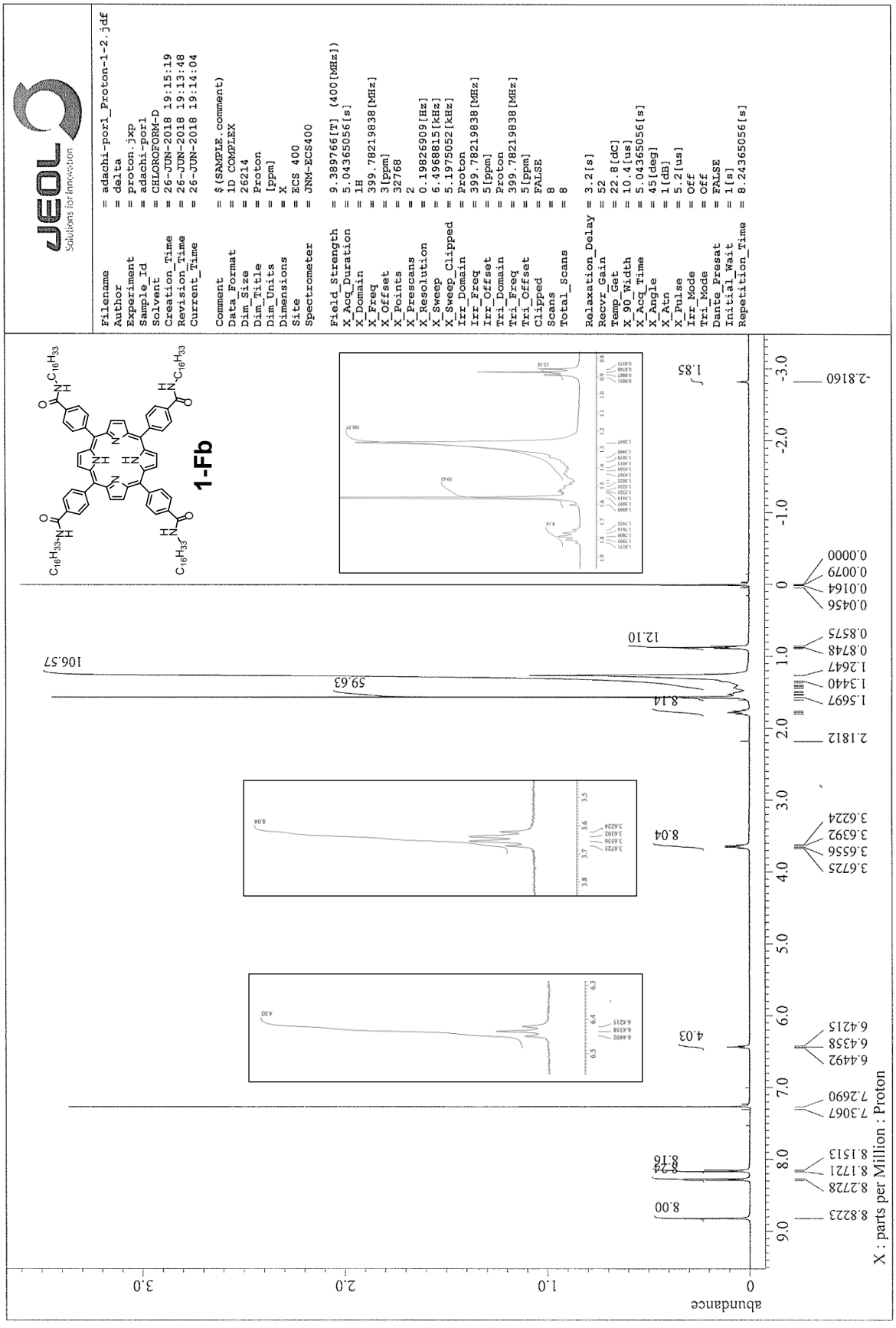

Figure S13. ^{1}H NMR spectra of **1-Fb** ($CDCl_3$, 400 MHz)

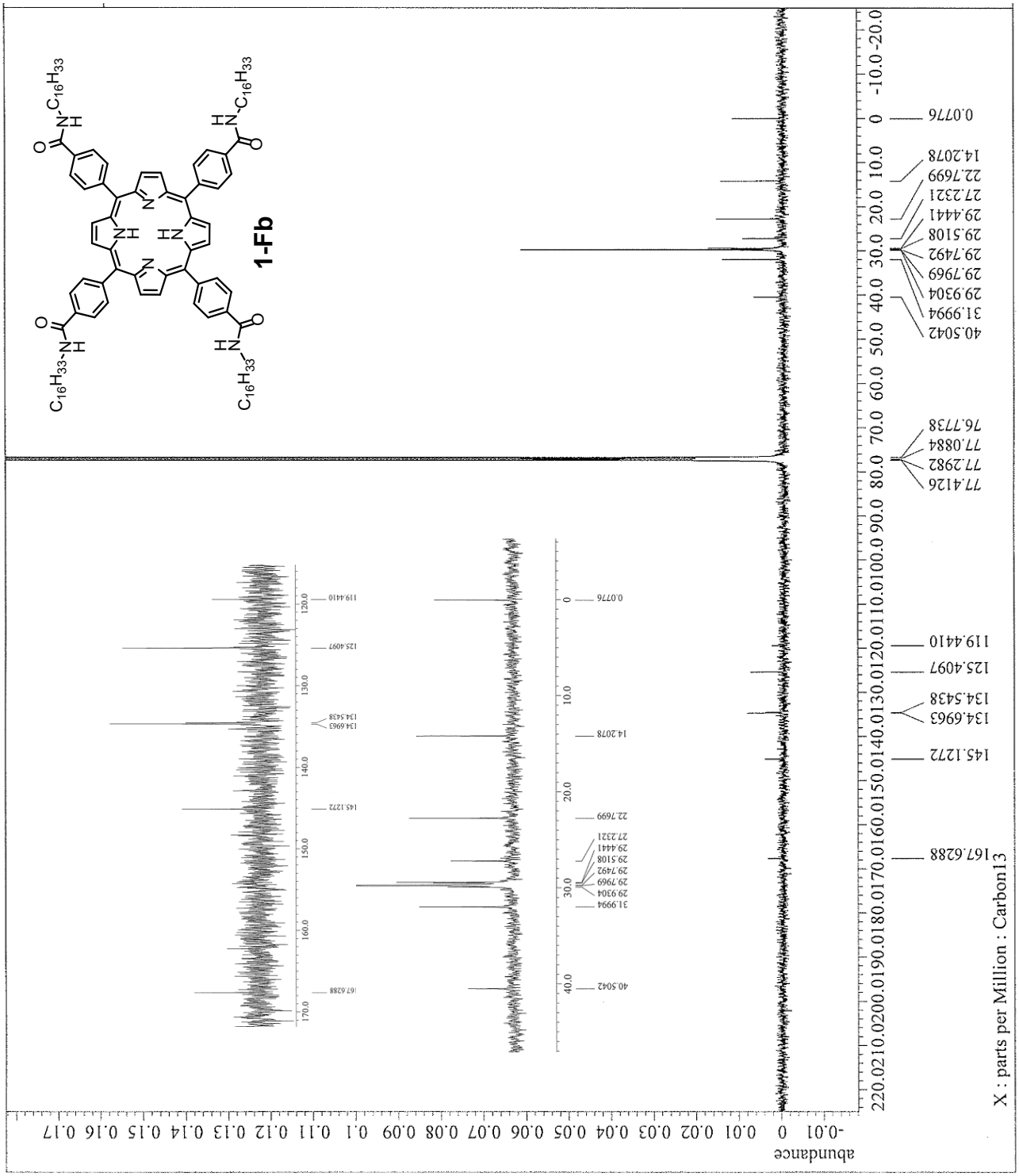

Figure S14. ^{13}C NMR spectra of **1-Fb** ($CDCl_3$, 101 MHz)

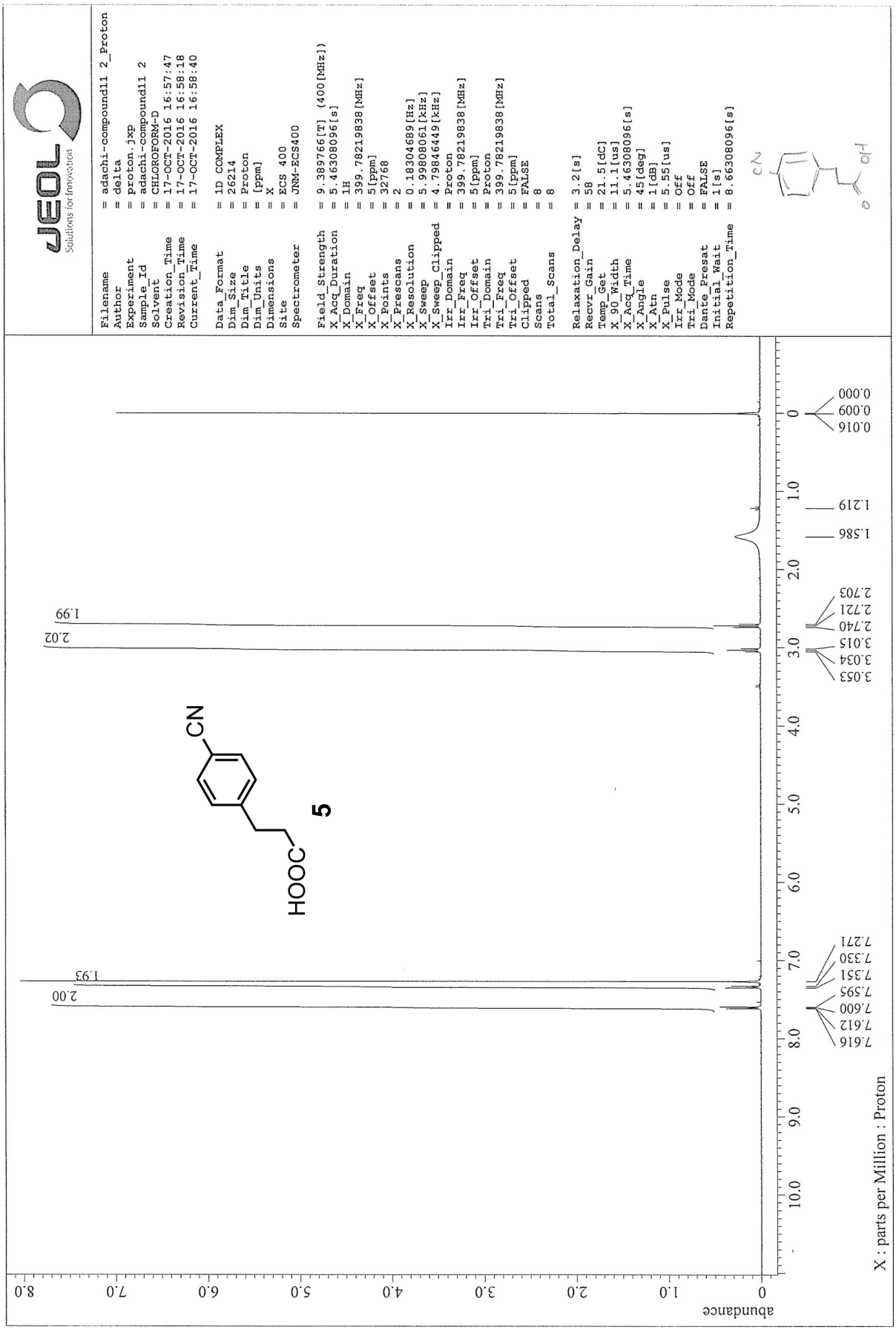

Figure S15. ^{1}H NMR spectra of **5** ($CDCl_3$, 400 MHz)

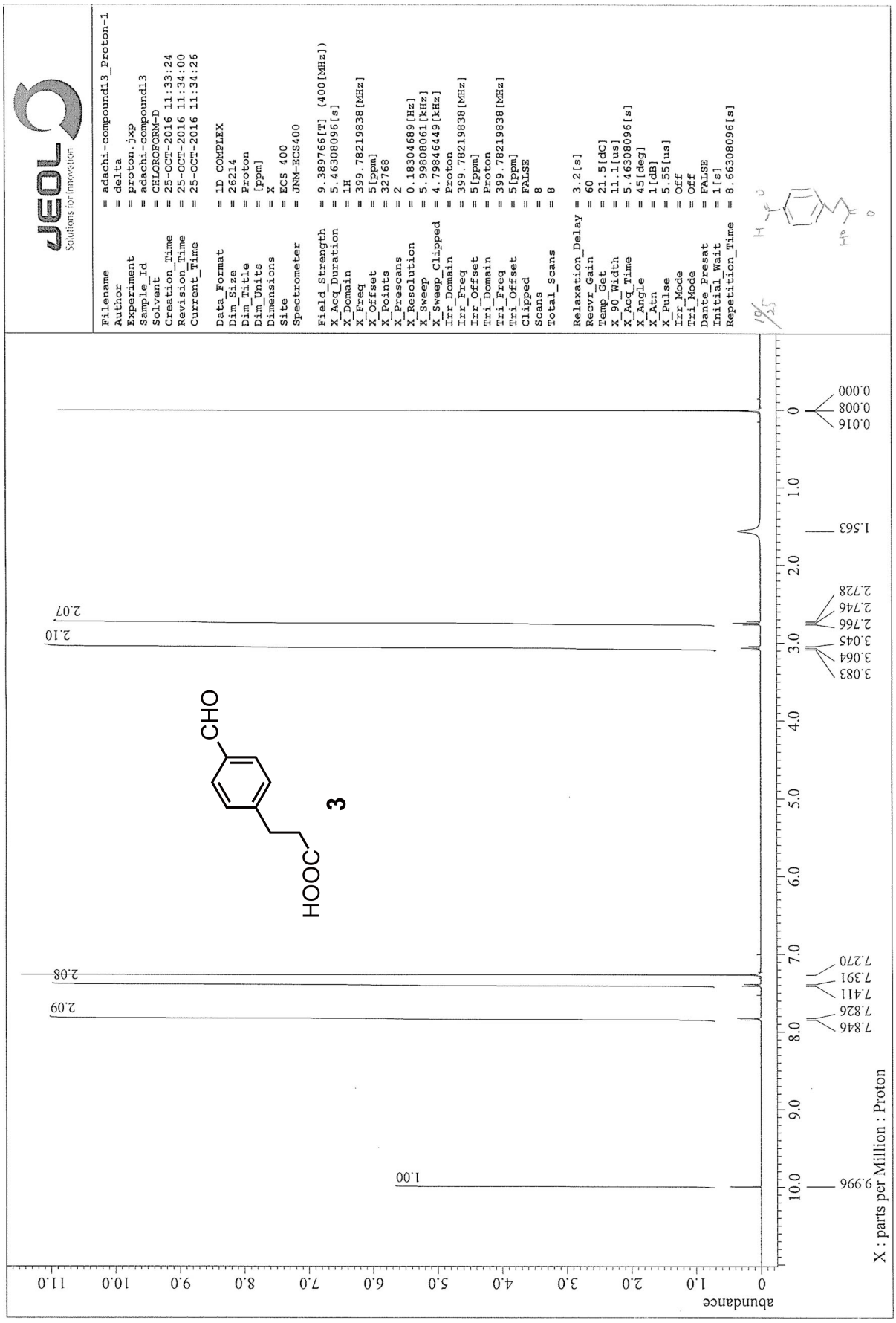

Figure S16. ^{1}H NMR spectra of **3** ($CDCl_3$, 400 MHz)

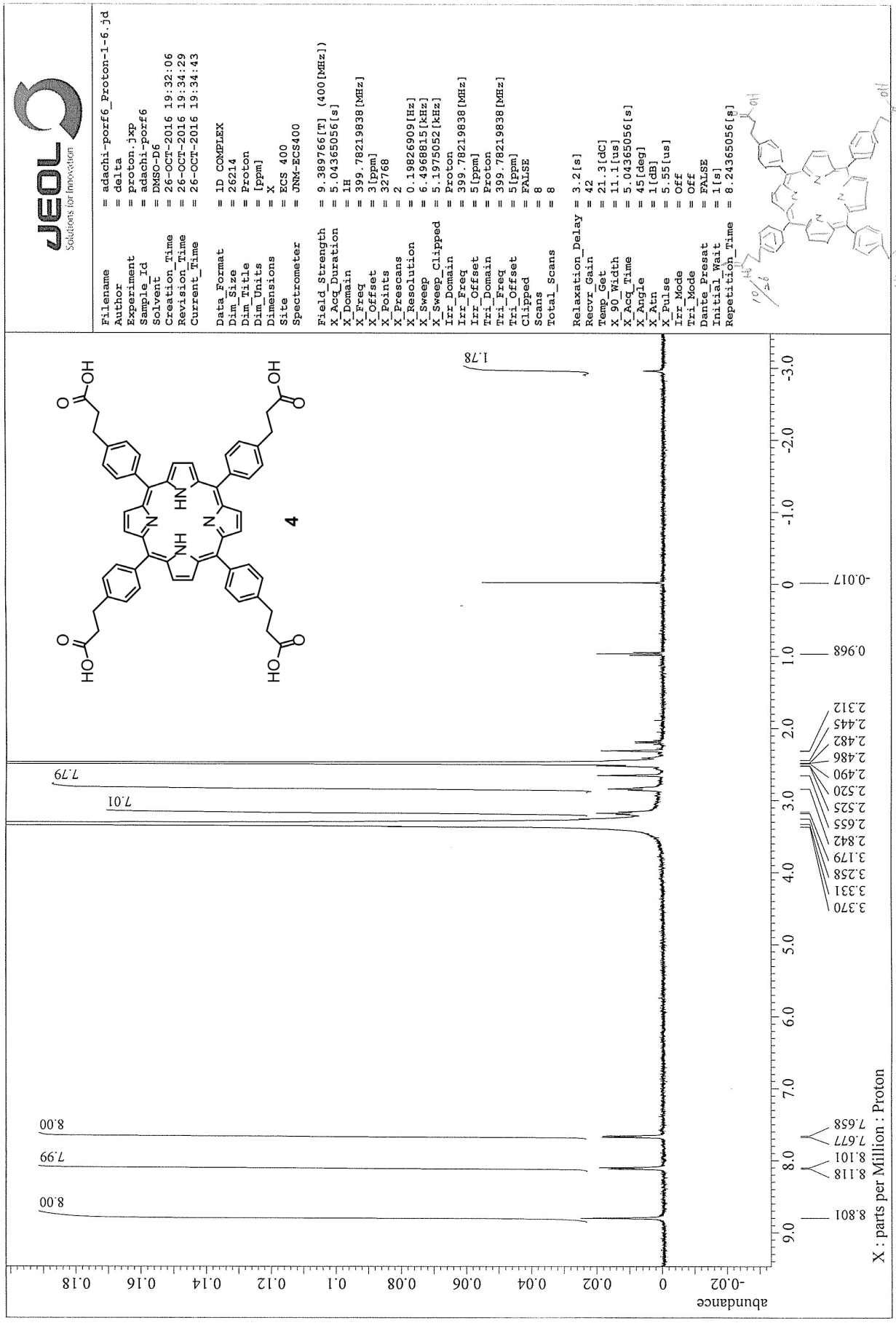

Figure S17. ^{1}H NMR of **4** ($CDCl_3$, 400 MHz)

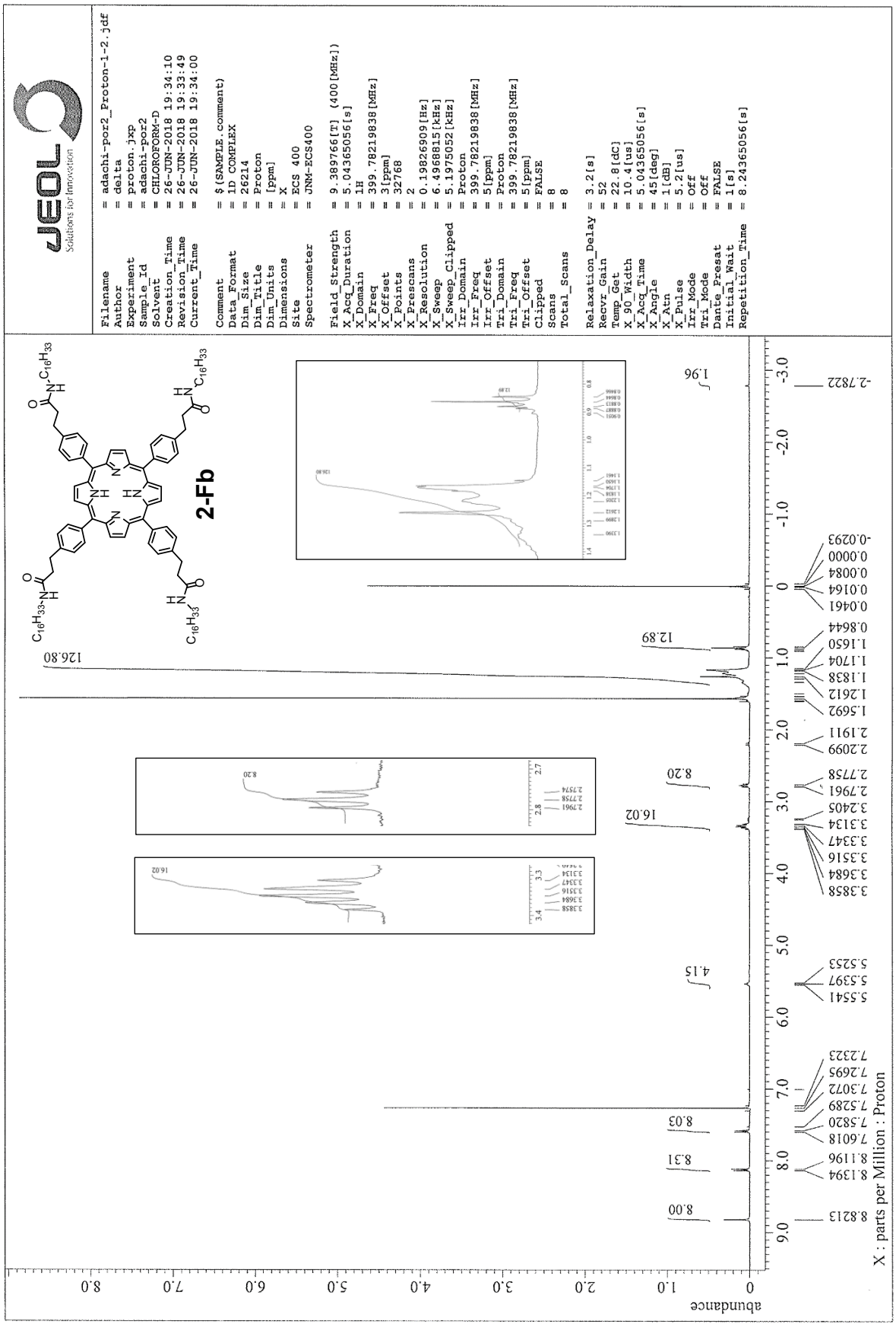

Figure S18. ^{1}H NMR spectra of **2-Fb** ($CDCl_3$, 400 MHz)

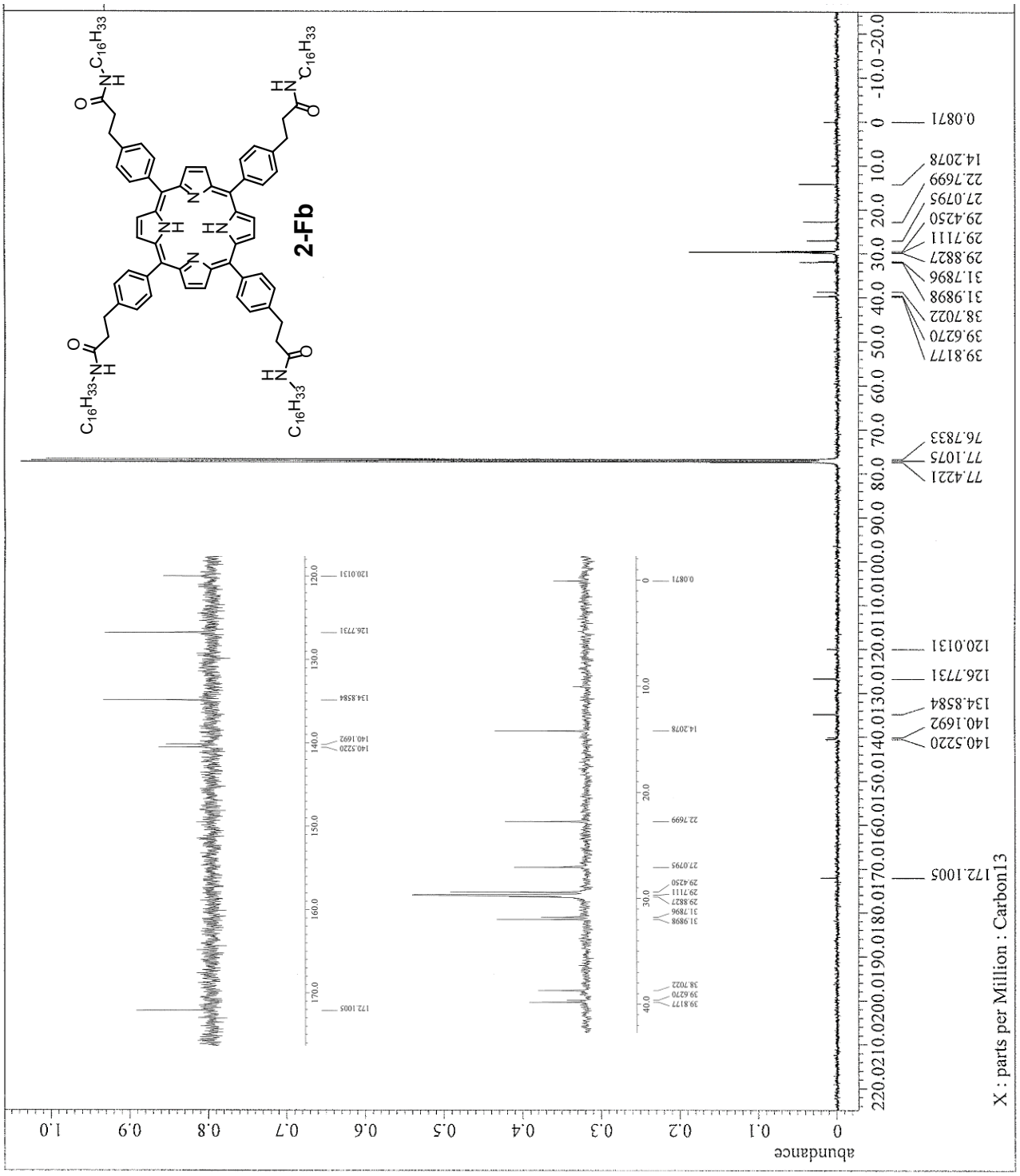

Figure S19. ^{13}C NMR spectra of **2-Fb** ($CDCl_3$, 101 MHz)

References

[S1] T. Sakanoi, J.-y. Hasegawa, K. Higashiguchi and K. Matsuda, *Chem. Asian J.* **2012**, *7*, 394–399.

[S2] S. Yokoyama, T. Hirose and K. Matsuda, *Chem. Commun.* **2014**, *50*, 5964–5966.

[S3] N. R. Vautravers and B. Breit, *Synlett* **2011**, *17*, 2517–2520.